

**Observation of  $B^0 \rightarrow D^{*-} \tau^+ \nu_\tau$  Decay at Belle**

A. Matyja,<sup>27</sup> M. Rozanska,<sup>27</sup> I. Adachi,<sup>8</sup> H. Aihara,<sup>41</sup> V. Aulchenko,<sup>1</sup> T. Aushev,<sup>18,13</sup> S. Bahinipati,<sup>3</sup> A. M. Bakich,<sup>37</sup> V. Balagura,<sup>13</sup> E. Barberio,<sup>21</sup> I. Bedny,<sup>1</sup> V. Bhardwaj,<sup>33</sup> U. Bitenc,<sup>14</sup> A. Bondar,<sup>1</sup> A. Bozek,<sup>27</sup> M. Bračko,<sup>20,14</sup> J. Brodzicka,<sup>8</sup> T. E. Browder,<sup>7</sup> M.-C. Chang,<sup>4</sup> P. Chang,<sup>26</sup> A. Chen,<sup>24</sup> K.-F. Chen,<sup>26</sup> B. G. Cheon,<sup>6</sup> R. Chistov,<sup>13</sup> I.-S. Cho,<sup>46</sup> Y. Choi,<sup>36</sup> Y. K. Choi,<sup>36</sup> J. Dalseno,<sup>21</sup> M. Dash,<sup>45</sup> S. Eidelman,<sup>1</sup> S. Fratina,<sup>14</sup> N. Gabyshev,<sup>1</sup> B. Golob,<sup>19,14</sup> H. Ha,<sup>16</sup> J. Haba,<sup>8</sup> T. Hara,<sup>32</sup> K. Hayasaka,<sup>22</sup> M. Hazumi,<sup>8</sup> D. Heffernan,<sup>32</sup> T. Hokuue,<sup>22</sup> Y. Hoshi,<sup>39</sup> W.-S. Hou,<sup>26</sup> H. J. Hyun,<sup>17</sup> T. Iijima,<sup>22</sup> K. Ikado,<sup>22</sup> K. Inami,<sup>22</sup> A. Ishikawa,<sup>41</sup> H. Ishino,<sup>42</sup> R. Itoh,<sup>8</sup> Y. Iwasaki,<sup>8</sup> H. Kaji,<sup>22</sup> S. Kajiwara,<sup>32</sup> J. H. Kang,<sup>46</sup> N. Katayama,<sup>8</sup> H. Kawai,<sup>2</sup> T. Kawasaki,<sup>29</sup> H. Kichimi,<sup>8</sup> Y. J. Kim,<sup>5</sup> K. Kinoshita,<sup>3</sup> S. Korpar,<sup>20,14</sup> Y. Kozakai,<sup>22</sup> P. Križan,<sup>19,14</sup> P. Krokovny,<sup>8</sup> R. Kumar,<sup>33</sup> C. C. Kuo,<sup>24</sup> Y.-J. Kwon,<sup>46</sup> J. S. Lee,<sup>36</sup> S. E. Lee,<sup>35</sup> T. Lesiak,<sup>27</sup> S.-W. Lin,<sup>26</sup> Y. Liu,<sup>5</sup> D. Liventsev,<sup>13</sup> F. Mandl,<sup>11</sup> S. McOnie,<sup>37</sup> T. Medvedeva,<sup>13</sup> K. Miyabayashi,<sup>23</sup> H. Miyake,<sup>32</sup> H. Miyata,<sup>29</sup> Y. Miyazaki,<sup>22</sup> R. Mizuk,<sup>13</sup> T. Mori,<sup>22</sup> Y. Nagasaka,<sup>9</sup> I. Nakamura,<sup>8</sup> M. Nakao,<sup>8</sup> Z. Natkaniec,<sup>27</sup> S. Nishida,<sup>8</sup> O. Nitoh,<sup>44</sup> T. Nozaki,<sup>8</sup> S. Ogawa,<sup>38</sup> T. Ohshima,<sup>22</sup> S. Okuno,<sup>15</sup> S. L. Olsen,<sup>7</sup> H. Ozaki,<sup>8</sup> P. Pakhlov,<sup>13</sup> G. Pakhlova,<sup>13</sup> H. Palka,<sup>27</sup> H. Park,<sup>17</sup> K. S. Park,<sup>36</sup> R. Pestotnik,<sup>14</sup> L. E. Piilonen,<sup>45</sup> Y. Sakai,<sup>8</sup> O. Schneider,<sup>18</sup> J. Schümann,<sup>8</sup> C. Schwanda,<sup>11</sup> A. J. Schwartz,<sup>3</sup> K. Senyo,<sup>22</sup> M. E. Sevier,<sup>21</sup> M. Shapkin,<sup>12</sup> C. P. Shen,<sup>10</sup> H. Shibuya,<sup>38</sup> S. Shinomiya,<sup>32</sup> J.-G. Shiu,<sup>26</sup> J. B. Singh,<sup>33</sup> A. Sokolov,<sup>12</sup> A. Somov,<sup>3</sup> S. Stanič,<sup>30</sup> M. Starič,<sup>14</sup> K. Sumisawa,<sup>8</sup> T. Sumiyoshi,<sup>43</sup> O. Tajima,<sup>8</sup> F. Takasaki,<sup>8</sup> M. Tanaka,<sup>8</sup> G. N. Taylor,<sup>21</sup> Y. Teramoto,<sup>31</sup> K. Trabelsi,<sup>8</sup> S. Uehara,<sup>8</sup> Y. Unno,<sup>6</sup> S. Uno,<sup>8</sup> P. Urquijo,<sup>21</sup> Y. Ushiroda,<sup>8</sup> G. Varner,<sup>7</sup> K. E. Varvell,<sup>37</sup> K. Vervink,<sup>18</sup> S. Villa,<sup>18</sup> C. C. Wang,<sup>26</sup> C. H. Wang,<sup>25</sup> P. Wang,<sup>10</sup> Y. Watanabe,<sup>15</sup> E. Won,<sup>16</sup> B. D. Yabsley,<sup>37</sup> A. Yamaguchi,<sup>40</sup> Y. Yamashita,<sup>28</sup> M. Yamauchi,<sup>8</sup> Z. P. Zhang,<sup>34</sup> and A. Zupanc<sup>14</sup>

(Belle Collaboration)

<sup>1</sup>*Budker Institute of Nuclear Physics, Novosibirsk*<sup>2</sup>*Chiba University, Chiba*<sup>3</sup>*University of Cincinnati, Cincinnati, Ohio 45221*<sup>4</sup>*Department of Physics, Fu Jen Catholic University, Taipei*<sup>5</sup>*The Graduate University for Advanced Studies, Hayama*<sup>6</sup>*Hanyang University, Seoul*<sup>7</sup>*University of Hawaii, Honolulu, Hawaii 96822*<sup>8</sup>*High Energy Accelerator Research Organization (KEK), Tsukuba*<sup>9</sup>*Hiroshima Institute of Technology, Hiroshima*<sup>10</sup>*Institute of High Energy Physics, Chinese Academy of Sciences, Beijing*<sup>11</sup>*Institute of High Energy Physics, Vienna*<sup>12</sup>*Institute of High Energy Physics, Protvino*<sup>13</sup>*Institute for Theoretical and Experimental Physics, Moscow*<sup>14</sup>*J. Stefan Institute, Ljubljana*<sup>15</sup>*Kanagawa University, Yokohama*<sup>16</sup>*Korea University, Seoul*<sup>17</sup>*Kyungpook National University, Taegu*<sup>18</sup>*Swiss Federal Institute of Technology of Lausanne, EPFL, Lausanne*<sup>19</sup>*University of Ljubljana, Ljubljana*<sup>20</sup>*University of Maribor, Maribor*<sup>21</sup>*University of Melbourne, School of Physics, Victoria 3010*<sup>22</sup>*Nagoya University, Nagoya*<sup>23</sup>*Nara Women's University, Nara*<sup>24</sup>*National Central University, Chung-li*<sup>25</sup>*National United University, Miao Li*<sup>26</sup>*Department of Physics, National Taiwan University, Taipei*<sup>27</sup>*H. Niewodniczanski Institute of Nuclear Physics, Krakow*<sup>28</sup>*Nippon Dental University, Niigata*<sup>29</sup>*Niigata University, Niigata*<sup>30</sup>*University of Nova Gorica, Nova Gorica*<sup>31</sup>*Osaka City University, Osaka*<sup>32</sup>*Osaka University, Osaka*<sup>33</sup>*Panjab University, Chandigarh*<sup>34</sup>*University of Science and Technology of China, Hefei*

<sup>35</sup>Seoul National University, Seoul<sup>36</sup>Sungkyunkwan University, Suwon<sup>37</sup>University of Sydney, Sydney, New South Wales<sup>38</sup>Toho University, Funabashi<sup>39</sup>Tohoku Gakuin University, Tagajo<sup>40</sup>Tohoku University, Sendai<sup>41</sup>Department of Physics, University of Tokyo, Tokyo<sup>42</sup>Tokyo Institute of Technology, Tokyo<sup>43</sup>Tokyo Metropolitan University, Tokyo<sup>44</sup>Tokyo University of Agriculture and Technology, Tokyo<sup>45</sup>Virginia Polytechnic Institute and State University, Blacksburg, Virginia 24061<sup>46</sup>Yonsei University, Seoul

(Received 29 June 2007; published 9 November 2007)

We report an observation of the decay  $B^0 \rightarrow D^{*-} \tau^+ \nu_\tau$  in a data sample containing  $535 \times 10^6 B\bar{B}$  pairs collected with the Belle detector at the KEKB asymmetric-energy  $e^+e^-$  collider. We find a signal with a significance of  $5.2\sigma$  and measure the branching fraction  $\mathcal{B}(B^0 \rightarrow D^{*-} \tau^+ \nu_\tau) = (2.02_{-0.37}^{+0.40}(\text{stat}) \pm 0.37(\text{syst}))\%$ . This is the first observation of an exclusive  $B$  decay with a  $b \rightarrow c\tau\nu_\tau$  transition.

DOI: 10.1103/PhysRevLett.99.191807

PACS numbers: 13.20.He, 14.80.Cp

$B$  meson decays with  $b \rightarrow c\tau\nu_\tau$  transitions can provide important constraints on the standard model (SM) and its extensions. Because of the large mass of the lepton in the final state these decays are sensitive probes of models with extended Higgs sectors [1] and provide observables sensitive to new physics, such as polarizations, which cannot be accessed in other semileptonic decays.

So far, results on semitauonic  $B$  decays are limited to inclusive and semi-inclusive measurements by LEP experiments [2] which measure an average branching fraction of  $\mathcal{B}(b \rightarrow \tau\nu_\tau X) = (2.48 \pm 0.26)\%$  [3]. SM calculations predict branching fractions for  $B \rightarrow \bar{D}^{*-} \tau^+ \nu_\tau$  around 1.4% [4].

In this Letter we present the first observation of  $B^0 \rightarrow D^{*-} \tau^+ \nu_\tau$  [5] decay using a data sample containing  $535 \times 10^6 B\bar{B}$  pairs that were collected with the Belle detector at the KEKB asymmetric-energy  $e^+e^-$  (3.5 on 8 GeV) collider [6] operating at the  $Y(4S)$  resonance ( $\sqrt{s} = 10.58$  GeV). The Belle detector is a large-solid-angle magnetic spectrometer consisting of a silicon vertex detector, a 50-layer central drift chamber, a system of aerogel Cherenkov counters, time-of-flight scintillation counters, and an electromagnetic calorimeter (ECL) comprised of CsI(Tl) crystals located inside a superconducting solenoid coil that provides a 1.5 T magnetic field. An iron flux return located outside the coil is instrumented to identify  $K_L^0$  mesons and muons. A detailed description of the detector can be found in Ref. [7]. We use Monte Carlo (MC) simulations to estimate signal efficiencies and background contributions. Large samples of the signal  $B^0 \rightarrow D^{*-} \tau^+ \nu_\tau$  decays are generated with the EVTGEN package [8] using the ISGW2 model [9]. Radiative effects are modeled by the PHOTOS code [10]. MC samples equivalent to about twice the accumulated data are used to evaluate the background from  $B\bar{B}$  and continuum  $q\bar{q}$  ( $q = u, d, s, c$ ) events.

$B$  decays to multineutrino final states can be observed at  $B$  factories via the recoil of the accompanying  $B$  meson ( $B_{\text{tag}}$ ) [11]. In this study we take advantage of the clean

signature provided by the  $D^*$  meson occurring on the signal side ( $B_{\text{sig}}$ ) and reconstruct the  $B_{\text{tag}}$  “inclusively” from all the particles that remain after selecting candidates for  $B_{\text{sig}}$  daughters. We apply the analysis to  $B_{\text{sig}}$  decay chains that combine a high reconstruction efficiency with a low background level. The  $D^{*-}$  mesons are reconstructed in the  $D^{*-} \rightarrow \bar{D}^0 \pi^-$  decay channel. The  $\bar{D}^0$ 's are reconstructed in the  $K^+ \pi^-$  and  $K^+ \pi^- \pi^0$  final states. The  $\tau^+ \rightarrow e^+ \nu_e \bar{\nu}_\tau$  and  $\tau^+ \rightarrow \pi^+ \bar{\nu}_\tau$  modes are used to reconstruct  $\tau$  lepton candidates. For the latter mode we analyze only the  $\bar{D}^0 \rightarrow K^+ \pi^-$  decay.

We select charged tracks with impact parameters that are consistent with an origin at the beam spot, and having momenta above 50 MeV/ $c$  in the laboratory frame. We assign masses using information from particle identification subsystems. The electrons from signal decays are selected with an efficiency greater than 90% and a misidentification rate below 0.2%. The momenta of particles identified as electrons are corrected for bremsstrahlung by adding photons within a 50 mrad cone along the trajectory. The  $\pi^0$  candidates are reconstructed from photon pairs having invariant mass in the range  $118 \text{ MeV}/c^2 < M_{\gamma\gamma} < 150 \text{ MeV}/c^2$ . To reduce the combinatorial background, we require photons from the  $\pi^0$  to have energies above 60–120 MeV, depending on the photon's polar angle. Photons that do not come from a  $\pi^0$  and exceed a polar-angle dependent energy threshold (100 MeV–200 MeV) are included in the  $B_{\text{tag}}$  reconstruction.

We reconstruct the signal decay by selecting combinations of a  $D^{*-}$  meson and an electron or a pion candidate with opposite charge. We accept  $\bar{D}^0$  candidates with invariant masses in a  $5\sigma$  window around the nominal Particle Data Group (PDG) [3] value.  $D^{*-}$  candidates are accepted if the mass difference  $M_{D^*} - M_{D^0}$  is in a  $3\sigma$  window around the PDG value.

Once a  $B_{\text{sig}}$  candidate is found, the remaining particles are used to reconstruct the  $B_{\text{tag}}$  decay. The consistency of a

$B_{\text{tag}}$  candidate with a  $B$ -meson decay is checked using the beam-energy constrained mass and the energy difference variables:  $M_{\text{tag}} = \sqrt{E_{\text{beam}}^2 - \mathbf{p}_{\text{tag}}^2}$ ,  $\mathbf{p}_{\text{tag}} \equiv \sum_i \mathbf{p}_i$ , and  $\Delta E_{\text{tag}} = E_{\text{tag}} - E_{\text{beam}}$ ,  $E_{\text{tag}} \equiv \sum_i E_i$ , where  $E_{\text{beam}}$  is the beam energy and  $\mathbf{p}_i$  and  $E_i$  denote the momentum vector and energy of the  $i$ th particle in the  $Y(4S)$  rest frame. The sum is over all particles that are not assigned to  $B_{\text{sig}}$  and satisfy the selection criteria described above. We require that events have at least one  $(D^{*-}e^+/\pi^+)$  pair,  $M_{\text{tag}} > 5.2 \text{ GeV}/c^2$  and  $|\Delta E_{\text{tag}}| < 0.6 \text{ GeV}$ . To improve the  $B_{\text{tag}}$  reconstruction, we impose the following requirements: zero total event charge, no  $\mu^\pm$  and no additional  $e^\pm$  in the event, zero net proton or antiproton number, residual energy in the ECL (i.e., the sum of energies of clusters that do not fulfill the requirements imposed on photons) less than 0.35 GeV, and the number of neutral particles on the tagging side  $N_{\pi^0} + N_\gamma < 5$ . These criteria, which we refer to as “the  $B_{\text{tag}}$  selection”, reject events in which some particles were undetected and suppress events with a large number of spurious showers. The  $B_{\text{tag}}$  simulation and reconstruction is validated using a control sample of events, where the  $B_{\text{sig}}$  decays to  $D^{*-}\pi^+$  (followed by  $D^{*-} \rightarrow \bar{D}^0\pi^-$ ,  $\bar{D}^0 \rightarrow K^+\pi^-$ ) which allows us to select a  $B\bar{B}$  sample with a purity of 96% and with  $B_{\text{sig}}$  and  $B_{\text{tag}}$  daughters properly assigned to the parent particles. Figure 1 shows the  $M_{\text{tag}}$  and  $\Delta E_{\text{tag}}$  distributions of the control sample for data and the MC simulation scaled to the integrated luminosity in data. The events satisfy the  $B_{\text{tag}}$ -selection criteria and are in the  $-0.25 \text{ GeV} < \Delta E_{\text{tag}} < 0.05 \text{ GeV}$  [for Fig. 1(a)] and  $M_{\text{tag}} > 5.27 \text{ GeV}/c^2$  [for Fig. 1(b)] windows. The good agreement of the shapes and of the absolute normalization demonstrates the validity of the MC simulations for  $B_{\text{tag}}$  decays. Based on this study we constrain all further analysis to the region  $-0.25 \text{ GeV} < \Delta E_{\text{tag}} < 0.05 \text{ GeV}$ .

The procedure described above, when applied to events with  $(D^{*-}e^+)$  pairs, selects a relatively clean sample of semileptonic  $B$  decays with the dominant nonsignal contribution from the  $B^0 \rightarrow D^{*-}e^+\nu_e$  mode. Combinatorial background from hadronic  $B$  decays dominates in the

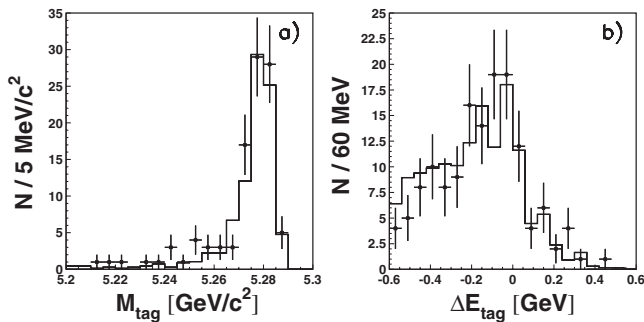


FIG. 1.  $M_{\text{tag}}$  and  $\Delta E_{\text{tag}}$  distributions for the  $B^0 \rightarrow D^{*-}\pi^+$  control sample from data (points with error bars) and MC (histograms).

$\tau^+ \rightarrow \pi^+\bar{\nu}_\tau$  mode. The background suppression exploits observables that characterize the signal decay: missing energy  $E_{\text{mis}} = E_{\text{beam}} - E_{D^*} - E_{e/\pi}$ , the sum of the energies of all particles in the event  $E_{\text{vis}}$ , the square of missing mass  $M_{\text{mis}}^2 = E_{\text{mis}}^2 - (\mathbf{p}_{\text{sig}} - \mathbf{p}_{D^*} - \mathbf{p}_{e/\pi})^2$ , and the effective mass of the  $(\tau^+\nu_\tau)$  pair,  $M_W^2 = (E_{\text{beam}} - E_{D^*})^2 - (\mathbf{p}_{\text{sig}} - \mathbf{p}_{D^*})^2$ , where  $\mathbf{p}_{\text{sig}} = -\mathbf{p}_{\text{tag}}$ . The most powerful variable for separating signal and background is obtained by combining  $E_{\text{mis}}$  and  $(D^*e/\pi)$  pair momentum:  $X_{\text{mis}} \equiv (E_{\text{mis}} - |\mathbf{p}_{D^*} + \mathbf{p}_{e/\pi}|) / \sqrt{E_{\text{beam}}^2 - m_{B^0}^2}$ , where  $m_{B^0}$  is the  $B^0$  mass. The  $X_{\text{mis}}$  variable is closely related to the missing mass in the  $B_{\text{sig}}$  decay. It lies in the range  $[-1, 1]$  for events with zero missing mass and takes larger values if there are multiple neutrinos. The MC distributions of  $X_{\text{mis}}$  and  $E_{\text{vis}}$  for signal and background events after  $B_{\text{tag}}$  selection for the  $\tau^+ \rightarrow e^+\nu_e\bar{\nu}_\tau$  mode are shown in Fig. 2. The relative normalizations of the main background categories,  $B^0 \rightarrow D^{*-}e^+\nu_e$ ,  $B \rightarrow D^{**}e^+\nu_e$ , other  $B$  decays, and  $q\bar{q}$  continuum, are determined from the data using looser selection criteria and verified using the sideband regions of the data sample that passed the final signal selection.

We optimize selection criteria using MC samples for signal and backgrounds, separately for decay chains with  $\tau^+ \rightarrow e^+\nu_e\bar{\nu}_\tau$  and with  $\tau^+ \rightarrow \pi^+\bar{\nu}_\tau$ . In the first case we require  $X_{\text{mis}} > 2.75$ ,  $1.9 \text{ GeV} < E_{\text{mis}} < 2.6 \text{ GeV}$ , and  $E_{\text{vis}} < 8.3 \text{ GeV}$ . We also reject events with a small difference between  $M_W^2$  and  $M_{\text{mis}}^2$  to suppress background from hadronic  $B$  decays where a genuine  $D^*$  meson is combined with a soft secondary  $e^\pm$ . Decays in the  $\tau^+ \rightarrow \pi^+\bar{\nu}_\tau$  mode are selected by requiring  $X_{\text{mis}} > 1.5$ ,  $M_W^2 - M_{\text{mis}}^2 - m_\tau^2 + m_\pi^2 > 0$  ( $m_\tau$  and  $m_\pi$  denote the masses of the  $\tau$  and charged  $\pi$ , respectively),  $E_{\text{vis}} < 8.3 \text{ GeV}$ , the energy of the  $\pi^+$  from the  $(D^{*-}\pi^+)$  pair greater than 0.6 GeV, no  $K_L^0$  in the event and less than four tracks that do not satisfy the requirements imposed on the impact parameters. The second requirement is equivalent to the condition  $|\cos\theta_{\nu_1\nu_2}| < 1$ , where  $\theta_{\nu_1\nu_2}$  denotes the angle between

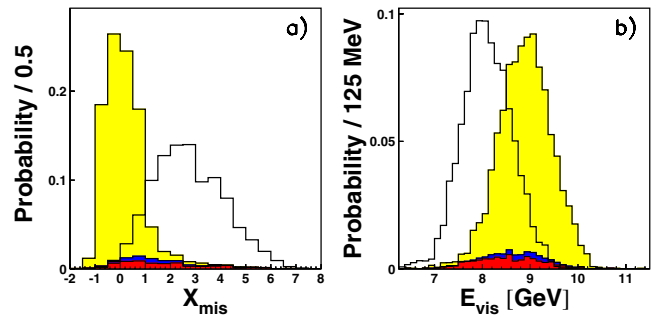


FIG. 2 (color online).  $X_{\text{mis}}$  and  $E_{\text{vis}}$  distributions (normalized to unity) after the  $B_{\text{tag}}$  selection for signal (blank) and background (shaded) for the  $\tau^+ \rightarrow e^+\nu_e\bar{\nu}_\tau$  mode in the region  $M_{\text{tag}} > 5.27 \text{ GeV}/c^2$ . The background components, from top to bottom:  $B^0 \rightarrow D^{*-}e^+\nu_e$ ,  $B \rightarrow D^{**}e^+\nu_e$ , and other  $B$  decays. The contribution from  $q\bar{q}$  continuum is negligible.

the two neutrinos in the  $(\tau^+ \nu_\tau)$  rest frame. The last three criteria reduce combinatorial background from low momentum pions and background from hadronic  $B \rightarrow D^{*-} K_L^0 + X$  and  $B \rightarrow D^{*-} n\bar{n} + X$  decays. The above requirements result in flat  $M_{\text{tag}}$  distributions for most background components, while the signal distribution remains unchanged. This allows us to use the  $M_{\text{tag}}$  variable to extract the signal.

The  $M_{\text{tag}}$  distribution of the signal is described using a Crystal Ball (CB) line shape function [12]. The shape parameters of the CB function are determined from unbinned maximum likelihood fits to the combined MC signal samples. All the fits are performed in the range  $M_{\text{tag}} > 5.2$  GeV/ $c^2$ . The backgrounds are modeled as the sum of a combinatorial component using a parametrization introduced by ARGUS (the ARGUS function) [13] and a peaking background described by the CB function with shape parameters fixed from the fit to the signal MC samples. The main source of the peaking background is the semileptonic decay  $B^0 \rightarrow D^{*-} e^+ \nu_e$ . Cross-feed events from signal decays followed by  $\tau$  decays to other modes are negligible in the  $\tau^+ \rightarrow e^+ \nu_e \bar{\nu}_\tau$  mode, but give significant contributions to the  $\tau^+ \rightarrow \pi^+ \bar{\nu}_\tau$  mode. We parametrize the  $M_{\text{tag}}$  distribution of cross-feed events as a sum of CB and ARGUS functions with shape parameters fixed from fits to the signal and combinatorial background as described above. The component described by the CB function is treated as a part of the signal. The efficiencies of signal reconstruction and the expected combinatorial and peaking backgrounds are given in Table I.

The selection criteria established in the MC studies are applied to the data. The resulting  $M_{\text{tag}}$  distribution for data in all three decay chains is shown in Fig. 3. The overlaid histogram represents the expected background, scaled to the data luminosity. A clear excess over background can be observed.

We extract signal yields by fitting the  $M_{\text{tag}}$  distributions to the sum of the expected signal and background distributions using the following likelihood function:

$$\mathcal{L} = e^{-(N_s + N_p + N_b)} \prod_{i=1}^N [(N_s + N_p) P_s(x_i) + N_b P_b(x_i)], \quad (1)$$

TABLE I. The number of expected combinatorial ( $N_b^{\text{MC}}$ ) and peaking ( $N_p$ ) background events, number of signal ( $N_s$ ) and combinatorial background ( $N_b$ ) events determined by the fits, number of events in data ( $N_{\text{obs}}$ ), signal selection efficiencies ( $\epsilon$ ), the product of the intermediate branching fractions ( $B$ ), extracted branching fraction for  $B^0 \rightarrow D^{*-} \tau^+ \nu_\tau$  ( $\mathcal{B}$ ), statistical significance ( $\Sigma$ ), and signal purity  $S \equiv N_s / (N_s + N_b + N_p)$  in the  $M_{\text{tag}} > 5.27$  GeV/ $c^2$  region.  $N_s$ ,  $\epsilon$ , and  $B$  in the  $\tau^+ \rightarrow \pi^+ \bar{\nu}_\tau$  mode include cross-feed events. The listed errors are statistical only.

Subchannel	$N_b^{\text{MC}}$	$N_p$	$N_s$	$N_b$	$N_{\text{obs}}$	$\epsilon \times 10^{-4}$	$B \times 10^{-3}$	$\mathcal{B}(\%)$	$\Sigma$	$S$
$\bar{D}^0 \rightarrow K^+ \pi^-$ , $\tau^+ \rightarrow e^+ \nu_e \bar{\nu}_\tau$	$26.3^{+3.4}_{-3.7}$	$1.2^{+1.6}_{-1.5}$	$19.5^{+5.8}_{-5.0}$	$19.4^{+5.8}_{-5.0}$	40	$3.25 \pm 0.11$	4.59	$2.44^{+0.74}_{-0.65}$	$5.0\sigma$	0.79
$\bar{D}^0 \rightarrow K^+ \pi^- \pi^0$ , $\tau^+ \rightarrow e^+ \nu_e \bar{\nu}_\tau$	$50.8^{+5.5}_{-5.1}$	$5.0^{+2.6}_{-2.2}$	$11.9^{+6.0}_{-5.2}$	$43.1^{+8.0}_{-7.2}$	60	$0.78 \pm 0.07$	17.03	$1.69^{+0.84}_{-0.74}$	$2.6\sigma$	0.50
$\bar{D}^0 \rightarrow K^+ \pi^-$ , $\tau^+ \rightarrow \pi^+ \bar{\nu}_\tau$	$138.0^{+9.2}_{-8.8}$	$-1.0^{+3.6}_{-3.2}$	$29.9^{+10.0}_{-9.1}$	$118.0^{+14.0}_{-13.0}$	148	$1.07^{+0.17}_{-0.15}$	25.72	$2.02^{+0.68}_{-0.61}$	$3.8\sigma$	0.48
Combined	$215^{+12}_{-11}$	$6.2^{+4.7}_{-4.2}$	$60^{+12}_{-11}$	$182^{+15}_{-14}$	248	$1.17^{+0.10}_{-0.08}$	47.34	$2.02^{+0.40}_{-0.37}$	$6.7\sigma$	0.57

where  $x_i$  is the  $M_{\text{tag}}$  in the  $i$ th event and  $N$  is the total number of events in the data.  $P_s$  ( $P_b$ ) denotes the signal (background) probability density function (PDF), which is parametrized as a CB (ARGUS) function with shape parameters determined from fits to MC samples and  $N_s$ ,  $N_b$ , and  $N_p$  are the numbers of signal, combinatorial background, and peaking background, respectively.  $N_s$  and  $N_b$  are free parameters of the fit, while  $N_p$  is fixed to the value obtained from fits to MC samples and scaled to the data luminosity ( $N_p$  is set to zero for the  $\tau^+ \rightarrow \pi^+ \bar{\nu}_\tau$  mode). The fits are performed both for the three decay chains separately and for all chains combined with a constraint to a common value of  $\mathcal{B}(B^0 \rightarrow D^{*-} \tau^+ \nu_\tau)$ . The fit results are included in Table I. The total number of signal events is  $60^{+12}_{-11}$  with a statistical significance of  $6.7\sigma$ . The significance is defined as  $\Sigma = \sqrt{-2 \ln(\mathcal{L}_0 / \mathcal{L}_{\text{max}})}$ , where  $\mathcal{L}_{\text{max}}$  and  $\mathcal{L}_0$  denote the maximum likelihood value and the likelihood value for the zero signal hypothesis. The fitted signal yield is used to calculate the branching fraction for the decay  $B^0 \rightarrow D^{*-} \tau^+ \nu_\tau$  using the following formula, which assumes equal fractions of charged and neutral  $B$  mesons produced in  $Y(4S)$  decays:  $\mathcal{B} = N_s / (N_{B\bar{B}} \times \sum_{ij} \epsilon_{ij} B_{ij})$ , where  $N_{B\bar{B}}$  is the number of  $B\bar{B}$  pairs,  $\epsilon_{ij}$  denotes the reconstruction efficiency of the specific decay chain, and  $B_{ij}$  is the product of intermediate branching fractions  $\mathcal{B}(D^{*-} \rightarrow \bar{D}^0 \pi^-) \times \mathcal{B}(\bar{D}^0 \rightarrow i) \times \mathcal{B}(\tau^+ \rightarrow j)$  [3]. The branching fraction obtained is  $\mathcal{B}(B^0 \rightarrow D^{*-} \tau^+ \nu_\tau) = (2.02^{+0.40}_{-0.37}(\text{stat}))\%$ .

As a consistency check we also use the  $M_{\text{mis}}^2$  and  $\cos\theta_{\nu_1 \nu_2}$  (for the  $\tau^+ \rightarrow \pi^+ \bar{\nu}_\tau$  mode) variables to extract the signal yield. We perform fits to distributions of these variables in the region  $M_{\text{tag}} > 5.27$  GeV/ $c^2$  and obtain branching fractions in the range 1.83%–2.05% and in agreement with the results from the  $M_{\text{tag}}$  fit.

We consider the following sources of systematic uncertainties in the branching fraction determination. The systematic error on  $N_{B\bar{B}}$  is 1.3%. The systematic error due to the statistical uncertainties in the CB shape is 2.8%. The CB parameters obtained from MC samples are, within statistical errors, consistent with those extracted from fits to the control sample in data. Therefore, we do not intro-

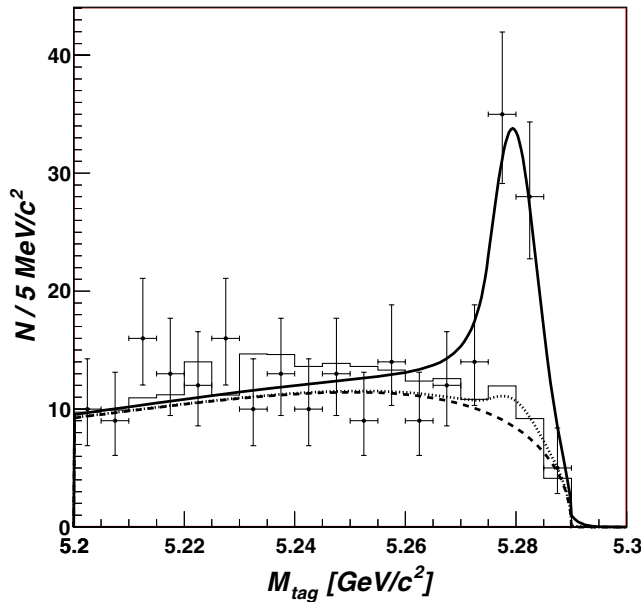


FIG. 3 (color online).  $M_{\text{tag}}$  distribution for the combined data sample. The histogram represents expected background scaled to the data luminosity. The solid curve shows the result of the fit. The dotted and dashed curves indicate, respectively, the fitted background and the component described by the ARGUS function.

duce additional uncertainties due to imperfect signal shape modeling. The systematic errors due to the parametrization of the combinatorial background are evaluated by changing the ARGUS-shape parameters by  $\pm 1\sigma$ . Fits with the shape parameters allowed to float provide consistent results within statistical uncertainties. The total systematic uncertainty due to the combinatorial background parametrization is  $^{+5.7}_{-10.1}\%$ . The systematic error due to the peaking background is evaluated for each channel and amounts to  $^{+8.2}_{-4.4}\%$  for combined modes, which is dominated by MC statistics. The uncertainty in  $B_{\text{tag}}$  reconstruction is taken as the statistical error in the  $B_{\text{tag}}$  efficiency evaluated from the data control sample (tagged with  $B^0 \rightarrow D^{*-}\pi^+$  decay) and is 10.9%. The systematic error on the determination of  $(D^{*-}e^+/\pi^+)$  pair selection efficiency comes from systematic uncertainties in the tracking efficiency, neutral reconstruction efficiency, and particle identification and is in the range 7.9%–10.7% depending on the decay chain. Systematic uncertainties in the signal selection efficiency are determined by comparing MC and data distributions in the variables used for signal selection. The uncertainties due to the partial branching ratios are taken from the errors quoted in PDG [3]. All of the above sources of systematic uncertainties are combined together taking into account correlations between different decay chains. The combined systematic uncertainty is 18.5%.

We include the effect of systematic uncertainty in the signal yield on the significance of the observed signal by

convolving the likelihood function from the fit with a Gaussian systematic error distribution. The significance of the observed signal after including systematic uncertainties is  $5.2\sigma$ .

In conclusion, in a sample of  $535 \times 10^6 B\bar{B}$  pairs we observe a signal of  $60^{+12}_{-11}$  events for the decay  $B^0 \rightarrow D^{*-}\tau^+\nu_\tau$  with a significance of  $5.2\sigma$ . This is the first observation of an exclusive  $B$  decay with the  $b \rightarrow c\tau\nu_\tau$  transition. The measured branching fraction:  $\mathcal{B}(B^0 \rightarrow D^{*-}\tau^+\nu_\tau) = (2.02^{+0.40}_{-0.37}(\text{stat}) \pm 0.37(\text{syst}))\%$  is consistent within experimental uncertainties with SM expectations [4].

We thank the KEKB group for excellent operation of the accelerator, the KEK cryogenics group for efficient solenoid operations, and the KEK computer group and the NII for valuable computing and Super-SINET network support. We acknowledge support from MEXT and JSPS (Japan); ARC and DEST (Australia); NSFC and KIP of CAS (China); DST (India); MOEHRD, KOSEF and KRF (Korea); KBN (Poland); MES and RFAAE (Russia); ARRS (Slovenia); SNSF (Switzerland); NSC and MOE (Taiwan); and DOE (USA).

- 
- [1] H. Itoh, S. Komine, and Y. Okada, *Prog. Theor. Phys.* **114**, 179 (2005), and references quoted therein.
  - [2] G. Abbiendi *et al.* (OPAL Collaboration), *Phys. Lett. B* **520**, 1 (2001); R. Barate *et al.* (ALEPH Collaboration), *Eur. Phys. J. C* **19**, 213 (2001); P. Abreu *et al.* (DELPHI Collaboration), *Phys. Lett. B* **496**, 43 (2000); M. Acciarri *et al.* (L3 Collaboration), *Z. Phys. C* **71**, 379 (1996).
  - [3] W.-M. Yao *et al.* (Particle Data Group), *J. Phys. G* **33**, 1 (2006).
  - [4] J.G. Körner and G.A. Schuler, *Phys. Lett. B* **231**, 306 (1989); D.S. Hwang and D.W. Kim, *Eur. Phys. J. C* **14**, 271 (2000); C.-H. Chen and C.-Q. Geng, *Phys. Rev. D* **71**, 077501 (2005).
  - [5] Throughout this Letter, the inclusion of the charge conjugate mode decay is implied unless otherwise stated.
  - [6] S. Kurokawa and E. Kikutani, *Nucl. Instrum. Methods Phys. Res., Sect. A* **499**, 1 (2003), and other papers included in this volume.
  - [7] A. Abashian *et al.* (Belle Collaboration), *Nucl. Instrum. Methods Phys. Res., Sect. A* **479**, 117 (2002).
  - [8] D.J. Lange, *Nucl. Instrum. Methods Phys. Res., Sect. A* **462**, 152 (2001).
  - [9] D. Scora and N. Isgur, *Phys. Rev. D* **52**, 2783 (1995).
  - [10] E. Barberio and Z. Wąs, *Comput. Phys. Commun.* **79**, 291 (1994).
  - [11] K. Ikado *et al.* (Belle Collaboration), *Phys. Rev. Lett.* **97**, 251802 (2006).
  - [12] T. Skwarnicki, Ph.D. thesis, Institute of Nuclear Physics, 1986; DESY Internal Report No. DESY F31-86-02, 1986.
  - [13] H. Albrecht *et al.* (ARGUS Collaboration), *Phys. Lett. B* **241**, 278 (1990).